Published in final edited form as:
*Tissue Eng Part A*. 2009 May ; 15(5): 1119–1125. doi:10.1089/ten.tea.2008.0162.

# Chemoattraction of Progenitor Cells by Remodeling Extracellular Matrix Scaffolds

**Allison J. Beattie, Ph.D.**[1], **Thomas W. Gilbert, Ph.D.**[1], **Juan Pablo Guyot, M.D.**[2], **Adolph J. Yates**[3], and **Stephen F. Badylak, D.V.M., M.D., Ph.D.**[1]

[1]McGowan Institute for Regenerative Medicine, University of Pittsburgh, Pittsburgh, Pennsylvania

[2]Department of Orthopaedic Surgery, Austral University Hospital, Buenos Aires, Argentina

[3]Department of Orthopaedic Surgery, University of Pittsburgh Medical Center, Pittsburgh, Pennsylvania

## Abstract

The chemotactic properties of a biologic scaffold composed of extracellular matrix (ECM) and subjected to *in vivo* degradation and remodeling were evaluated in a mouse model of Achilles tendon reconstruction. Following a segmental resection of the Achilles tendon in both C57BL/6 and MRL/MpJ mice, the defect was repaired with either an ECM scaffold composed of urinary bladder matrix (UBM) or resected autologous tendon. The surgically repaired and the contralateral tendons were harvested at 3, 7, and 14 days following surgery from each animal. Chemotaxis of multipotential progenitor cells toward the harvested tissue was quantified using a fluorescent-based cell migration assay. Results showed greater migration of progenitor cells toward tendons repaired with UBM–ECM scaffold compared to both the tendons repaired with autologous tissue and the normal contralateral tendon in both the MRL/MpJ and C57BL/6 mice. The magnitude and temporal pattern of the chemotactic response differed between the two mouse strains.

## Introduction

The extracellular matrix (ECM) of mammalian tissues is a complex three-dimensional network of molecules that provides both structural support and biologic signals for cell adhesion, migration, and proliferation. The degradation of ECM molecules and the subsequent release of cryptic matrikines are important events in the matrix remodeling process, and these bioactive molecules play an important role in both physiological and pathological events. Many studies have shown that ECM molecules such as collagen, when subjected to proteolytic degradation, release matrikines (cryptic segments of larger proteins) that possess bioactivity, which is distinct from that of the parent molecule, including bacteriostasis, chemotaxis, and mitogenesis.[1,2] Peptides released from laminin, collagen, elastin, and fibronectin are known to participate in the modulation of cellular activities, mellaprotease matrix metalloprotease (MMP) expression, and growth factor signaling.[3] Cleavage of the ECM molecule laminin has been attributed to the progression of malignant tumors by stimulating the migration of tumorigenic cells[5] and metastasis associated with proteolytically modified ECM.[6,7] ECM degradation products also participate in tumor vascularization,[8] and matrikines produced by matrix MMP digestion are known to release molecules that stimulate angiogenesis during wound healing



Address reprint requests to: Stephen F. Badylak, D.V.M., M.D., Ph.D., McGowan Institute for Regenerative Medicine, University of Pittsburgh, 100 Technology Drive, Suite 200, Pittsburgh, PA 15219, badylaks@upmc.edu.

and embryogenesis by promoting migration of endothelial cells.[9] Therefore, the phenomenon of bioactive degradation products is not novel.

Biologic scaffolds composed of naturally occurring ECM derived from tissues such as the urinary bladder (UBM) and small intestine have been successfully used as scaffolds for the reconstruction of several tissue types in both preclinical studies[10-13] and clinical applications.[14-18] ECM scaffolds contain the same structural and functional proteins, glycoproteins, and proteoglycans that are present in native ECM and are therefore responsive to the same ECM proteases. It has been shown that ECM scaffolds that are not chemically crosslinked are degraded completely with 60–90 days and rapidly infiltrated by host cells.[19-21] The host tissue that forms concomitant with or following degradation consists of site-specific tissue as opposed to scar tissue.[22] The mechanisms behind this altered host response to injury are not fully understood, but are thought to be related to the release of matricryptic peptides during degradation of the scaffold.

ECM scaffolds that are degraded *in vitro* by non-physiologic methods (heat and acid) release products that have been shown to possess bacteriostatic and chemotactic properties.[23-26] It is important to note that scaffold degradation is essential to realize the bacteriostatic properties since the intact scaffold materials can support bacterial growth *in vitro*.[27] The link between the *in vitro* and *in vivo* antimicrobial properties has been well established. ECM scaffolds have been shown to resist infection following deliberate bacterial contamination in preclinical studies[28,29] and spontaneous contamination in the clinical environment.[13,16,30] Conversely, chemically crosslinked ECM scaffolds that show inhibited degradation are contraindicated for infected sites in clinical use because they cannot resist chronic infection.

The link between the *in vitro* and *in vivo* chemotactic activity has yet to be established. Although several *in vivo* studies have shown that ECM scaffolds attract circulating bone marrow–derived cells that remain at the site of the remodeled host tissue,[31,32] this directed migration and accumulation of cells has not been directly linked to the presence of ECM degradation products.

The objective of the present study was to determine if the process of ECM scaffold degradation and remodeling that occurs *in vivo* is associated chemotaxis for a population of progenitor cells in a well-characterized *in vitro* assay.

## Overview of Experimental Design

Two strains of mice were used in this study: C57BL/6 mice and MRL/MpJ mice (Jackson Laboratories, Bar Harbor, ME). The MRL/MpJ strain was used for two reasons: (1) the cells used in the chemotactic assay were derived from this strain, and (2) the MRL mouse strain has been reported to be a regenerative mouse model, and cells that participate in the regenerative process have been characterized.[26] The C57BL/6 strain was used because it is representative of normal mammalian wound healing. Thirty-six mice of each strain were randomly divided into three equal groups of 12. A 2 mm segmental defect of Achilles tendon was created in the right hind leg of all animals in each group. The defect was repaired with an interpositional graft consisting of an ECM biologic scaffold (UBM–ECM) in half of the animals of each group (ECM-T), and autologous excised tendon tissue was used to repair the defect in the remaining animals (AUTO-T). Twelve mice of each strain were sacrificed at the following time points: 3, 7, or 14 days. The repaired tendon and contralateral normal tendon were excised from each animal at the time of sacrifice and identified as repaired and normal tendon from the mouse that received UBM repair (ECM-T and ECM-C, respectively), and repaired and normal tendon from the mouse that received the autologous tissue repair (AUTO-T and AUTO-C, respectively) (Table 1). The excised tissues were evaluated in an *in vitro* assay that quantified chemotactic activity for a population of multipotential progenitor cells.

## Materials and Methods

### UBM–ECM scaffold preparation

Biologic scaffolds composed of ECM derived from porcine urinary bladder (UBM–ECM) were prepared as described previously using techniques that simulate commercial processes.[11,33,34] Briefly, the basement membrane of the tunica epithelialis mucosa and subjacent tunica propria of the porcine urinary bladder, collectively termed urinary bladder matrix (UBM), were mechanically and chemically isolated from adjacent tissue layers, decellularized, and then disinfected by immersion in 0.1% (v/v) peracetic acid, 4% (v/v) ethanol, and 96% (v/v) deionized water for 2 h. The UBM–ECM material was washed twice for 15 min with PBS (pH 7.4) and then twice for 15 min with deionized water.

Three hydrated sheets of UBM–ECM were stacked in such a manner that the basement membrane was the outermost surface on both sides of the multilaminate sheet. This orientation of ECM layers assured that the relatively nonadherent basement membrane surface would always interface with the adjacent tissue and minimize adhesion formation.[35,36] The entire assembly was laminated by placing the three scaffold sheets between two perforated stainless steel plates, which were then sealed in vacuum bagging and subjected to a vacuum of 710–730 mmHg for approximately 8 h. The multilaminate device was cut into a 3×2 mm (length×width) section and terminally sterilized by exposure to ethylene oxide.

### Surgical procedure and tissue harvest

Mice were anesthetized with inhalant Isoflurane using a nose cone. The right hind limb of each animal was shaved and prepared for surgery using sterile techniques as previously described.[31] Under magnification, the right Achilles tendon was exposed through a posterolateral skin incision and the surrounding paratenon incised. Two 7–0 Vicryl sutures (Ethicon, Somerville, NJ) were placed proximal and distal in the Achilles tendon. The spacing of the two sutures was 3 mm. In the AUTO-T group ($n$=18) the proximal and distal sutures were placed through the intervening native tendon tissue creating two loops of suture. The tendon was then transected within each loop, creating the autologous tendon graft (Fig. 1). The two suture loops were pulled tight and knotted to secure the graft in the defect area. In the ECM-T group ($n$=18), a 2 mm segment of the tendon was resected and a 3×2 mm (length×width) triple layer laminated sheet of UBM–ECM was attached to the free ends of the tendon via the two placed sutures (Fig. 1). Prior to closing the skin, the graft was rehydrated with sterile saline and then tubularized around the free ends of the tendon. In both groups the wound was closed in layers using 7–0 Vicryl sutures. At the predetermined time of sacrifice for each animal, the surgically repaired tendon and the contralateral control tendon were harvested. The harvested tendons were immediately frozen on dry ice and stored at −80°C. All procedures were approved by the Institutional Animal Care and Use Committee at the University Pittsburgh and complied with the NIH Guidelines for the Care and Use of Laboratory Animals.

### Cell culture

The cells used in the chemotactic assay were harvested from MRL/MpJ mice. These cells were characterized as progenitor cells by their expression of Tenascin-C, *Thy-1*, *Dlk/Pref-1*, *Msx1*, Thrombospondin, and *Tbx5* (Fig. 2). These cells were harvested from the blastema structure that forms following hole punch in the ear of MRL/MpJ mice (Jackson Laboratories).[26] Briefly, a 2 mm hole was punched through the ear of MRL/MpJ mice.[37,38] Eleven days after creation of the ear hole, cells were isolated from the healing edge of the hole. After initial expansion, cells were maintained in Dulbecco's modified Eagle's medium (DMEM; Cat. No. D6429; Sigma-Aldrich, St. Louis, MO) supplemented with 10% fetal calf serum (FCS), 2 mM L-glutamine, 100 U/mL penicillin, and 100 μg/mL streptomycin in 95% air/5% $CO_2$. All cells used for these experiments were expanded in culture and used at passage 14.

### RNA isolation and analysis

Mouse MRL blastemal cells (MRL-B) were grown to at least 50% confluence in 75 $cm^2$ flasks, collected, and lysed. Total RNA was extracted using the Qiagen RNeasy Kit (Qiagen, Valencia, CA) per manufacturer's instructions with the recommended DNase treatment for removal of genomic DNA. RNA concentrations were determined by measuring absorbance at 260 nm on a BioMate3 spectrophotometer (Thermo Spectronic, Rochester, NY). Control RNA samples from human and mouse tissues were prepared by homogenization in TriReagent and chloroform extraction; RNA was extracted from aqueous phase using Qiagen RNeasy Kit as detailed above. First-strand cDNA was synthesized from 1 μg of RNA using the Superscript First-Strand Synthesis System according to the manufacturer's instructions (Invitrogen–Life Technologies, Carlsbad, CA). PCR was performed with primers specific for *Tbx-5*, *Msx-1*, *Pref-1* (Dlk), *Thy-1*, Tenascin C (TnC), Thrombospondin (THBS), and glyceraldehyde 3-phosphate dehydrogenase (*GAPDH*) (Table 2). cDNAs were amplified in EasyStart Micro100 tubes (Molecular BioProducts, San Diego, CA) with 100 nM of primer in a Mastercycler (Eppendorf, Westbury, NY). All PCR reactions were performed in 35 cycles. PCR products were separated on 2% agarose gels, stained with ethidium bromide, and visualized on Kodak Image Station 2000R (Kodak, Rochester, NY).

### Cell migration assay

Cell migration was measured using the CytoSelect™ cell migration assay (Cell Biolabs, San Diego, CA). Following a 20 h starvation period in 0.5% heat-inactivated serum in DMEM, cells were resuspended at $4\times10^5$ cells/mL in migration media (basal DMEM) and preincubated for 1 h in a 5% $CO_2$/95% air 37°C incubator. Each harvested tendon segment was dissected into three pieces of approximately equal size using a dissecting microscope. The weight of each tendon was determined and recorded prior to dissection. Each tendon piece was then placed in a separate well of a 96-well feeder tray containing 150 μL of migration media. One hundred and fifty microliters of assay controls, DMEM supplemented with 10% FCS (positive control) and basal DMEM (negative control), was also tested in triplicate. The migration tray, consisting of a 96-well membrane chamber with pores 8 μm in size, was placed into the feeder tray, and 100 μL of cell suspension (approximately 40,000 cells) was added to the top half of each well above the membrane. The tray was covered and incubated for 4 h at 37°C in 5% $CO_2$/95% air. Following the 4 h incubation, the migration tray was separated from the feeder tray, and cells that had failed to migrate were removed from the upper membrane chamber by aspiration. The migration tray, with migrated cells attached to the underside of the membrane, was placed into a harvesting tray containing 150 μL of prewarmed cell detachment solution and incubated in a cell culture incubator for 1 h. The migration chamber was removed from the harvesting tray, and 50 μL of cell lysis/dye solution, prepared by diluting CyQuant® GR dye in lysis buffer (1:75), was added to each well of the harvesting tray and then incubated at room temperature for 20 min. About 150 μL of the mixture from each well was transferred to a 96-well plate suitable for fluorescence measurement (Nunc™, Roskilde, Denmark). The fluorescence tag, bound to DNA fragments of migrated cells, was measured in a SpectraMax M2 Plate Reader (Molecular Devices, Sunnyvale, CA) at 480 nm/520 nm.

### Statistics

A four-factor repeated measures analysis of variance was performed (SAS Statistical Software v9.1.3; SAS Institute, Cary, NC) to determine effects of ECM treatment, repair, strain, and time. Results were considered significant at $p$-values less than 0.05.

## Results

### C57BL/6 mice

The mean weight of the tendon segments dissected from all C57BL/6 mice was 19.98 ± 8.51 mg ($n$=72). Tendons repaired with the UBM–ECM scaffold (ECM-T) excised from C57BL/6 mice showed chemotactic activity that was greater than either ECM-C or AUTO-T group at day 7, but not at days 3 or 14 (Fig. 3). At the day 7 time point the number of cells migrating toward ECM-T tendons was 49% greater than autologous repaired tendons (AUTO-T) and 54% greater than the contralateral normal tendons from the UBM receiving mouse (ECM-C).

### MRL/MpJ mice

The mean weight of the tendon segments dissected from all MRL/MpJ mice was 19.31 ± 9.26 mg ($n$=72). In the MRL mouse model the tendon that received the UBM–ECM scaffold (ECM-T) showed increased chemotactic activity for MRL-B cells at days 3 and 7 compared to ECM-C and AUTO-T groups ($p$<0.05), but not at day 14 (Fig. 3). No differences were detected between the AUTO-T and AUTO-C groups. The recruitment of cells for the ECM-T group increased relative to the AUTO-T (108% at day 3 and 36% at day 7) and ECM-C groups (90% at day 3 and 61% at day 7). There was a significant change in chemotactic activity with time for the ECM-T group, with the greatest activity at day 3, and decreasing activity with time at 7 and 14 days ($p$<0.05). There was a significant increase in cell recruitment to ECM-T from the MRL/MpJ strain as compared to the C57BL/6 strain ($p$<0.05).

## Discussion

The results of the present study show that there is positive chemotactic activity for a progenitor cell population, specifically MRL blastema cells, within the remodeling ECM scaffold material excised from Achilles tendons during the early stages of *in vivo* degradation and remodeling. The data showed that the degree and temporal pattern of the chemotactic activity is different in MRL/MpJ versus C57BL/6 mice.

The increased migration of progenitor cells toward the remodeling UBM–ECM scaffold in both mouse strains is likely the result of the release of soluble growth factors and matricryptic peptides that form during degradation. ECM scaffolds are known to contain various growth factors that retain their activity even after prolonged shelf life, including TGF-β, b-FGF, and VEGF.[39-42] The degradation of ECM scaffolds *in vivo* begins immediately after implantation[43,44] and is likely associated with the release of both intact proteins and cryptic fragments of parent molecules. It cannot be determined with certainty the extent to which the recruitment of progenitor cells shown in the present was due to soluble growth factors or matricryptic peptides. Recent studies have shown that *in vitro* degradation products of UBM–ECM scaffolds are chemotactic for human multi-lineage progenitor cells and MRL-blastema cells, the cells used in the present study.[26] It is unknown whether degradation products formed following the *in vivo* degradation process in the ECM-T remodeling tendons are of the same biochemical composition as those formed *in vitro* by Li *et al*.[23] and Reing *et al*.[26]

There is a difference in the chemotactic activity that was measured from the acellular ECM of the scaffold material compared to that measured for the autologous tendon tissue or the normal tendon. One possible explanation for this difference is that the decellularized UBM–ECM scaffold (by definition) lacks any intact cellular component at the time of implantation. In contrast, it is likely that cells in the autologous tendon graft are driven toward apoptosis or necrosis as a result of surgical devascularization and release of proinflammatory mediators. Recent studies that compared the host response to an ECM scaffold and an autologous muscle tissue graft for abdominal wall repair in a rat model showed that the remodeled autologous

tissue prompted a proinflammatory macrophage phenotype by 2 weeks after implantation, and the long-term outcome was scar tissue formation.[20,45,46] In contrast, the remodeled acellular ECM promoted an anti-inflammatory macrophage phenotype, which resulted in site-specific regeneration of muscle tissue.

A second possible explanation for differences in chemotactic activity between the UBM–ECM and autologous tendon involves the inherent differences between the ECM of tendons and the ECM of urinary bladder. The tendon is a metabolically stable tissue with limited collagen turnover, which allows it to maintain its mechanical strength. Due to the necessity for rapid healing, the ECM of the urinary bladder may have an evolutionary advantage over organs that remodel or heal more slowly. Furthermore, there may be fewer and different growth factors present within tendon ECM. Although several studies have isolated ECM from tendons,[47-50] there are no reports of *in vivo* remodeling of the harvested tendon ECM.

It is noteworthy that the ECM-T tendons explanted from the MRL mice showed greater chemotactic activity than ECM-T tendons explanted from the C57BL/6 mice at day 3. MRL mice have been described as having rapid healing and enhanced regenerative capability not found in most mammalian species.[37,51,52] The regenerative capacity of the MRL mouse was first realized when it was discovered that they spontaneously healed critical-sized ear punches without scar tissue formation,[38] although this finding appears to depend on the location and severity of the injury.[51,53] When regeneration occurs, the formation of multiple tissue types is associated with a blastema-like structure. The blastema-like structure is the source of the MRL-B cells that were used in the *in vitro* assay in the current study originate. Other tissues in the MRL mouse that may have regenerative capability include the heart, brain, and spinal cord.[52] The MRL mouse has also been reported to present an abnormal immune system. The relationship of the healing properties and differences in the immune system differences to the finding of our study are unknown and beyond the scope of the manuscript.

It has been shown that MRL mice have increased expression and activity of *MMP-2* and *MMP-9* in the early stages of healing of an ear punch as compared to C57BL/6 mice.[54] MRL mice have also been shown to more aggressively degrade basement membrane forms of ECM,[54] which is known to be a component of UBM–ECM.[36] It is possible that increased expression and activity of MMPs in the MRL/MpJ strain may lead to more rapid degradation than occurs in the C57BL/6 mouse, and thus an earlier release of chemotactic degradation products. Therefore, if indeed the release of matricryptic peptides were the main factor responsible for the recruitment of progenitor cells, it would be expected that the C57BL/6 would display a delayed response. The degradation of the ECM scaffolds was not quantitatively measured in the current study, so additional work will be required to determine whether the degradation profiles of the ECM scaffolds differ for the two strains.

The ECM did not appear to provide positive recruitment of progenitor cells at 14 days after implantation, regardless of the strain. Certainly, large portions of the scaffold are still present beyond 7 days, and this scaffold material continues to remodel. However, there is also an active host cellular response that is characterized by a phenotypically different population of cells, which may in turn affect the recruitment of progenitor cells. Therefore, the tissue tested from the 14-day explants represented a mixture of xenogeneic scaffold, newly deposited host tissue, and an abundance of host cells. Day 14 is the point at which the level of cellularity typically peaks during the remodeling of an ECM scaffold, after which point the degree of cellularity gradually decreases. The same mechanisms that explain this decrease in cellularity may also be responsible for the decreased recruitment of progenitor cells.

There are several limitations of the current study. First, the source of progenitor cells (MRL-blastema) chosen for the current study is native to one of the strains used for the *in vivo*

implantation, specifically the MRL/MpJ.[37,38,55] However, the remodeled UBM–ECM harvested from the surgical site in both mouse strains showed more chemotactic potential than the remodeled autologous tendon. Bone marrow–derived mononuclear cells would have been an interesting population to examine since it is known that bone marrow–derived cells are recruited to the site of ECM remodeling and become part of the tissue, but the specific population of marrow-derived cells to evaluate would have been an arbitrary choice. The specific populations of cells recruited to the site of ECM remodeling are an area of current interest. Finally, this study does not specifically identify the cell-specific enzymes that contribute to scaffold degradation in the Achilles tendon model.

## Conclusion

The *in vivo* process of UBM–ECM degradation and remodeling leads to the recruitment of progenitor cells to the site of remodeling. This recruitment is associated with the production and release of chemotactic molecules that may represent intact growth factors, matricryptic peptides, or both. The importance of these bioactive molecules in facilitating a constructive remodeling process is unknown, but this study establishes a link between the reports of chemotactic properties that result from *in vitro* methods of ECM scaffold degradation and the *in vivo* process of scaffold remodeling and recruitment of selected cell populations.

## References

1. Bellon G, Martiny L, Robinet A. Matrix metalloproteinases and matrikines in angiogenesis. Crit Rev Oncol Hematol 2004;49:203. [PubMed: 15036261]
2. Tran KT, Lamb P, Deng JS. Matrikines and matricryptins: implications for cutaneous cancers and skin repair. J Dermatol Sci 2005;40:11. [PubMed: 15993569]
3. Li YY, McTiernan CF, Feldman AM. Interplay of matrix metalloproteinases, tissue inhibitors of metalloproteinases and their regulators in cardiac matrix remodeling. Cardiovasc Res 2000;46:214. [PubMed: 10773225]
4. Plopper GE, Huff JL, Rust WL, Schwartz MA, Quaranta V. Antibody-induced activation of beta1 integrin receptors stimulates cAMP-dependent migration of breast cells on laminin-5. Mol Cell Biol Res Commun 2000;4:129. [PubMed: 11170844]
5. Ohtaka K, Watanabe S, Iwazaki R, Hirose M, Sato N. Role of extracellular matrix on colonic cancer cell migration and proliferation. Biochem Biophys Res Commun 1996;220:346. [PubMed: 8645308]
6. Mackay AR, Gomez DE, Nason AM, Thorgeirsson UP. Studies on the effects of laminin, E-8 fragment of laminin and synthetic laminin peptides PA22-2 and YIGSR on matrix metalloproteinases and tissue inhibitor of metalloproteinase expression. Lab Invest 1994;70:800. [PubMed: 8015284]
7. Stetler-Stevenson WG, Hewitt R, Corcoran M. Matrix metalloproteinases and tumor invasion: from correlation and causality to the clinic. Semin Cancer Biol 1996;7:147. [PubMed: 8773300]
8. Lochter A, Bissell MJ. Involvement of extracellular matrix constituents in breast cancer. Semin Cancer Biol 1995;6:165. [PubMed: 7495985]
9. Stupack DG, Cheresh DA. ECM remodeling regulates angiogenesis: endothelial integrins look for new ligands. Sci STKE 2002;2002:PE7. [PubMed: 11842241]
10. Badylak SF, Kochupura PV, Cohen IS, Doronin SV, Saltman AE, Gilbert TW, Kelly DJ, Ignotz RA, Gaudette GR. The use of extracellular matrix as an inductive scaffold for the partial replacement of functional myocardium. Cell Transplant 2006;15(Suppl 1):S29. [PubMed: 16826793]
11. Badylak SF, Vorp DA, Spievack AR, Simmons-Byrd A, Hanke J, Freytes DO, Thapa A, Gilbert TW, Nieponice A. Esophageal reconstruction with ECM and muscle tissue in a dog model. J Surg Res 2005;128:87. [PubMed: 15922361]
12. Hiles MC, Badylak SF, Lantz GC, Kokini K, Geddes LA, Morff RJ. Mechanical properties of xenogeneic small-intestinal submucosa when used as an aortic graft in the dog. J Biomed Mater Res 1995;29:883. [PubMed: 7593028]

13. Jernigan TW, Croce MA, Cagiannos C, Shell DH, Handorf CR, Fabian TC. Small intestinal submucosa for vascular reconstruction in the presence of gastrointestinal contamination. Ann Surg 2004;239:733. [PubMed: 15082978]
14. De Ugarte DA, Choi E, Weitzbuch H, Wulur I, Caulkins C, Wu B, Fonkalsrud EW, Atkinson JB, Dunn JC. Mucosal regeneration of a duodenal defect using small intestine submucosa. Am Surg 2004;70:49. [PubMed: 14964547]
15. Pu LL. Small intestinal submucosa (Surgisis) as a bioactive prosthetic material for repair of abdominal wall fascial defect. Plast Reconstr Surg 2005;115:2127. [PubMed: 15923867]
16. Shell, DHt; Croce, MA.; Cagiannos, C.; Jernigan, TW.; Edwards, N.; Fabian, TC. Comparison of small-intestinal submucosa and expanded polytetrafluoroethylene as a vascular conduit in the presence of gram-positive contamination. Ann Surg 2005;241:995. [PubMed: 15912049]
17. MacLeod TM, Sarathchandra P, Williams G, Sanders R, Green CJ. Evaluation of a porcine origin acellular dermal matrix and small intestinal submucosa as dermal replacements in preventing secondary skin graft contraction. Burns 2004;30:431. [PubMed: 15225907]
18. Sardeli C, Axelsen SM, Bek KM. Use of porcine small intestinal submucosa in the surgical treatment of recurrent rectocele in a patient with Ehlers-Danlos syndrome type III. Int Urogynecol J Pelvic Floor Dysfunct 2005;16:504. [PubMed: 15645146]
19. Badylak SF, Record R, Lindberg K, Hodde J, Park K. Small intestinal submucosa: a substrate for *in vitro* cell growth. J Biomater Sci Polym Ed 1998;9:863. [PubMed: 9724899]
20. Valentin JE, Badylak JS, McCabe GP, Badylak SF. Extracellular matrix bioscaffolds for orthopaedic applications: a comparative histologic study. J Bone Joint Surg Am 2006;88:2673. [PubMed: 17142418]
21. Gilbert TW, Stewart-Akers AM, Simmons-Byrd A, Badylak SF. Degradation and remodeling of small intestinal submucosa in canine Achilles tendon repair. J Bone Joint Surg Am 2007;89:621. [PubMed: 17332112]
22. Cobb MA, Badylak SF, Janas W, Boop FA. Histology after dural grafting with small intestinal submucosa. Surg Neurol 1996;46:389. [PubMed: 8876722]
23. Li F, Li W, Johnson S, Ingram D, Yoder M, Badylak S. Low-molecular-weight peptides derived from extracellular matrix as chemoattractants for primary endothelial cells. Endothelium 2004;11:199. [PubMed: 15370297]
24. Brennan EP, Reing J, Chew D, Myers-Irvin JM, Young EJ, Badylak SF. Antibacterial activity within degradation products of biological scaffolds composed of extracellular matrix. Tissue Eng 2006;12:2949. [PubMed: 17518662]
25. Sarikaya A, Record R, Wu CC, Tullius B, Badylak S, Ladisch M. Antimicrobial activity associated with extracellular matrices. Tissue Eng 2002;8:63. [PubMed: 11886655]
26. Reing JE, Zhang L, Myers-Irvin J, Cordero KE, Freytes DO, Heber-Katz E, Bedelbaeva K, McIntosh D, Dewilde A, Braunhut SJ, Badylak SF. Degradation products of extracellular matrix affect cell migration and proliferation. Tissue Eng. 2008In press
27. Holtom PD, Shinar Z, Benna J, Patzakis MJ. Porcine small intestine submucosa does not show antimicrobial properties. Clin Orthop Relat Res 2004;427:18. [PubMed: 15552130]
28. Badylak SF, Wu CC, Bible M, McPherson E. Host protection against deliberate bacterial contamination of an extracellular matrix bioscaffold versus Dacron mesh in a dog model of orthopedic soft tissue repair. J Biomed Mater Res B Appl Biomater 2003;67:648. [PubMed: 14528463]
29. Badylak SF, Coffey AC, Lantz GC, Tacker WA, Geddes LA. Comparison of the resistance to infection of intestinal submucosa arterial autografts versus polytetrafluoroethylene arterial prostheses in a dog model. J Vasc Surg 1994;19:465. [PubMed: 8126859]
30. Mantovani F, Trinchieri A, Castelnuovo C, Romano AL, Pisani E. Reconstructive urethroplasty using porcine acellular matrix. Eur Urol 2003;44:600. [PubMed: 14572761]
31. Zantop T, Gilbert TW, Yoder MC, Badylak SF. Extracellular matrix scaffolds are repopulated by bone marrow-derived cells in a mouse model of achilles tendon reconstruction. J Orthop Res 2006;24:1299. [PubMed: 16649228]
32. Badylak SF, Park K, Peppas N, McCabe G, Yoder M. Marrow-derived cells populate scaffolds composed of xenogeneic extracellular matrix. Exp Hematol 2001;29:1310. [PubMed: 11698127]

33. Freytes DO, Badylak SF, Webster TJ, Geddes LA, Rundell AE. Biaxial strength of multilaminated extracellular matrix scaffolds. Biomaterials 2004;25:2353. [PubMed: 14741600]
34. Kochupura PV, Azeloglu EU, Kelly DJ, Doronin SV, Badylak SF, Krukenkamp IB, Cohen IS, Gaudette GR. Tissue-engineered myocardial patch derived from extracellular matrix provides regional mechanical function. Circulation 2005;112:I144. [PubMed: 16159807]
35. Vracko R. Basal lamina scaffold-anatomy and significance for maintenance of orderly tissue structure. Am J Pathol 1974;77:314. [PubMed: 4614671]
36. Brown B, Lindberg K, Reing J, Stolz DB, Badylak SF. The basement membrane component of biologic scaffolds derived from extracellular matrix. Tissue Eng 2006;12:519. [PubMed: 16579685]
37. Heber-Katz E. The regenerating mouse ear. Semin Cell Dev Biol 1999;10:415. [PubMed: 10497098]
38. Clark LD, Clark RK, Heber-Katz E. A new murine model for mammalian wound repair and regeneration. Clin Immunol Immunopathol 1998;88:35. [PubMed: 9683548]
39. Hodde JP, Ernst DM, Hiles MC. An investigation of the long-term bioactivity of endogenous growth factor in OASIS Wound Matrix. J Wound Care 2005;14:23. [PubMed: 15656461]
40. Hodde JP, Record RD, Liang HA, Badylak SF. Vascular endothelial growth factor in porcine-derived extracellular matrix. Endothelium 2001;8:11. [PubMed: 11409848]
41. McDevitt CA, Wildey GM, Cutrone RM. Transforming growth factor-beta1 in a sterilized tissue derived from the pig small intestine submucosa. J Biomed Mater Res A 2003;67:637. [PubMed: 14566807]
42. Voytik-Harbin SL, Brightman AO, Kraine MR, Waisner B, Badylak SF. Identification of extractable growth factors from small intestinal submucosa. J Cell Biochem 1997;67:478. [PubMed: 9383707]
43. Baramova EN, Shannon JD, Bjarnason JB, Fox JW. Degradation of extracellular matrix proteins by hemorrhagic metalloproteinases. Arch Biochem Biophys 1989;275:63. [PubMed: 2817904]
44. Buckley S, Driscoll B, Shi W, Anderson K, Warburton D. Migration and gelatinases in cultured fetal, adult, and hyperoxic alveolar epithelial cells. Am J Physiol Lung Cell Mol Physiol 2001;281:L427. [PubMed: 11435218]
45. Badylak SF, Gilbert TW. Immune response to biologic scaffold materials. Semin Immunol 2008;20:109. [PubMed: 18083531]
46. Badylak SF, Valentin JE, Ravindra AK, McCabe GP, Stewart-Akers AM. Macrophage phenotype as a determinant of biologic scaffold remodeling. Tissue Eng. 2008In press
47. Faraj KA, van Kuppevelt TH, Daamen WF. Construction of collagen scaffolds that mimic the three-dimensional architecture of specific tissues. Tissue Eng 2007;13:2387. [PubMed: 17627479]
48. Tischer T, Vogt S, Aryee S, Steinhauser E, Adamczyk C, Milz S, Martinek V, Imhoff AB. Tissue engineering of the anterior cruciate ligament: a new method using acellularized tendon allografts and autologous fibroblasts. Arch Orthop Trauma Surg 2007;127:735. [PubMed: 17541614]
49. Whitlock PW, Smith TL, Poehling GG, Shilt JS, van Dyke M. A naturally derived, cytocompatible, and architecturally optimized scaffold for tendon and ligament regeneration. Biomaterials 2007;28:4321. [PubMed: 17610948]
50. Woods T, Gratzer PF. Effectiveness of three extraction techniques in the development of a decellularized bone-anterior cruciate ligament-bone graft. Biomaterials 2005;26:7339. [PubMed: 16023194]
51. Rajnoch C, Ferguson S, Metcalfe AD, Herrick SE, Willis HS, Ferguson MW. Regeneration of the ear after wounding in different mouse strains is dependent on the severity of wound trauma. Dev Dyn 2003;226:388. [PubMed: 12557217]
52. Leferovich JM, Bedelbaeva K, Samulewicz S, Zhang XM, Zwas D, Lankford EB, Heber-Katz E. Heart regeneration in adult MRL mice. Proc Natl Acad Sci USA 2001;98:9830. [PubMed: 11493713]
53. Beare AH, Metcalfe AD, Ferguson MW. Location of injury influences the mechanisms of both regeneration and repair within the MRL/MpJ mouse. J Anat 2006;209:547. [PubMed: 17005026]
54. Gourevitch D, Clark L, Chen P, Seitz A, Samulewicz SJ, Heber-Katz E. Matrix metalloproteinase activity correlates with blastema formation in the regenerating MRL mouse ear hole model. Dev Dyn 2003;226:377. [PubMed: 12557216]

55. Masinde G, Li X, Baylink DJ, Nguyen B, Mohan S. Isolation of wound healing/regeneration genes using restrictive fragment differential display-PCR in MRL/MPJ and C57BL/6 mice. Biochem Biophys Res Commun 2005;330:117. [PubMed: 15781240]

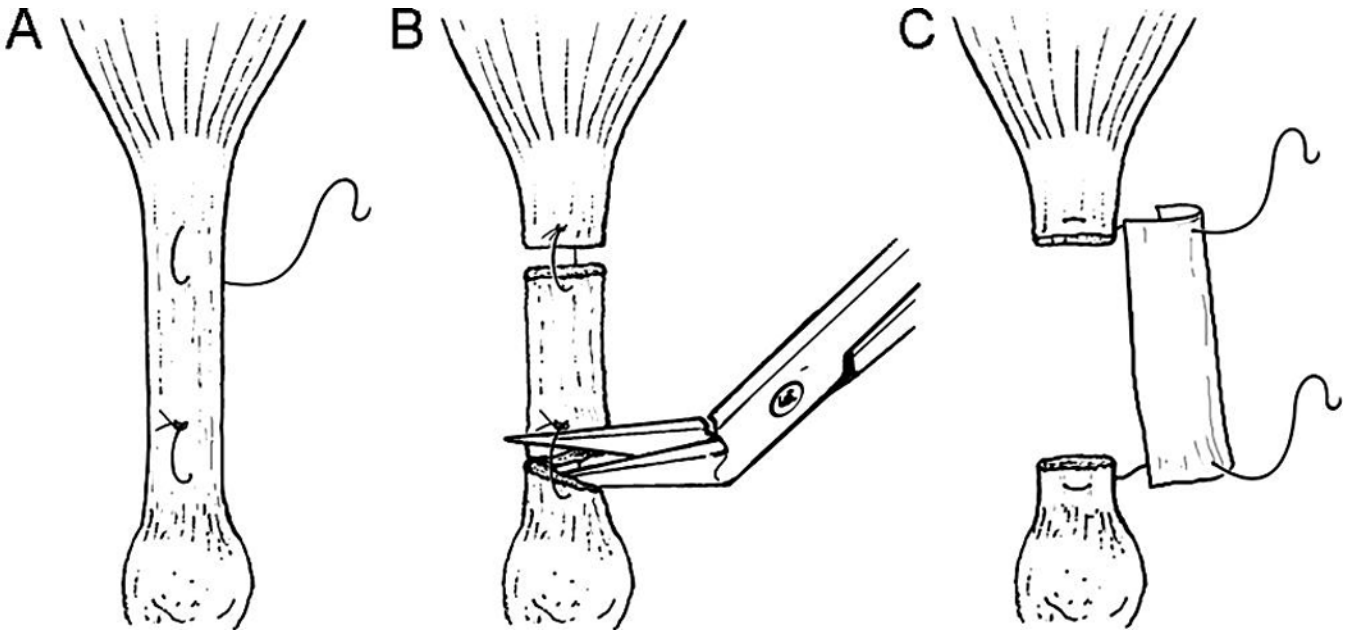


**FIG. 1.**

Schematic diagram illustrating the surgical technique used to transect the Achilles tendon in the autologous repair (AUTO-T) group. (**A**) Sutures placed prior to segmental excision. (**B**) Transection between loops of suture creating the autologous tendon repair. (**C**) Excision of tendon segment with placement of UBM–ECM material.

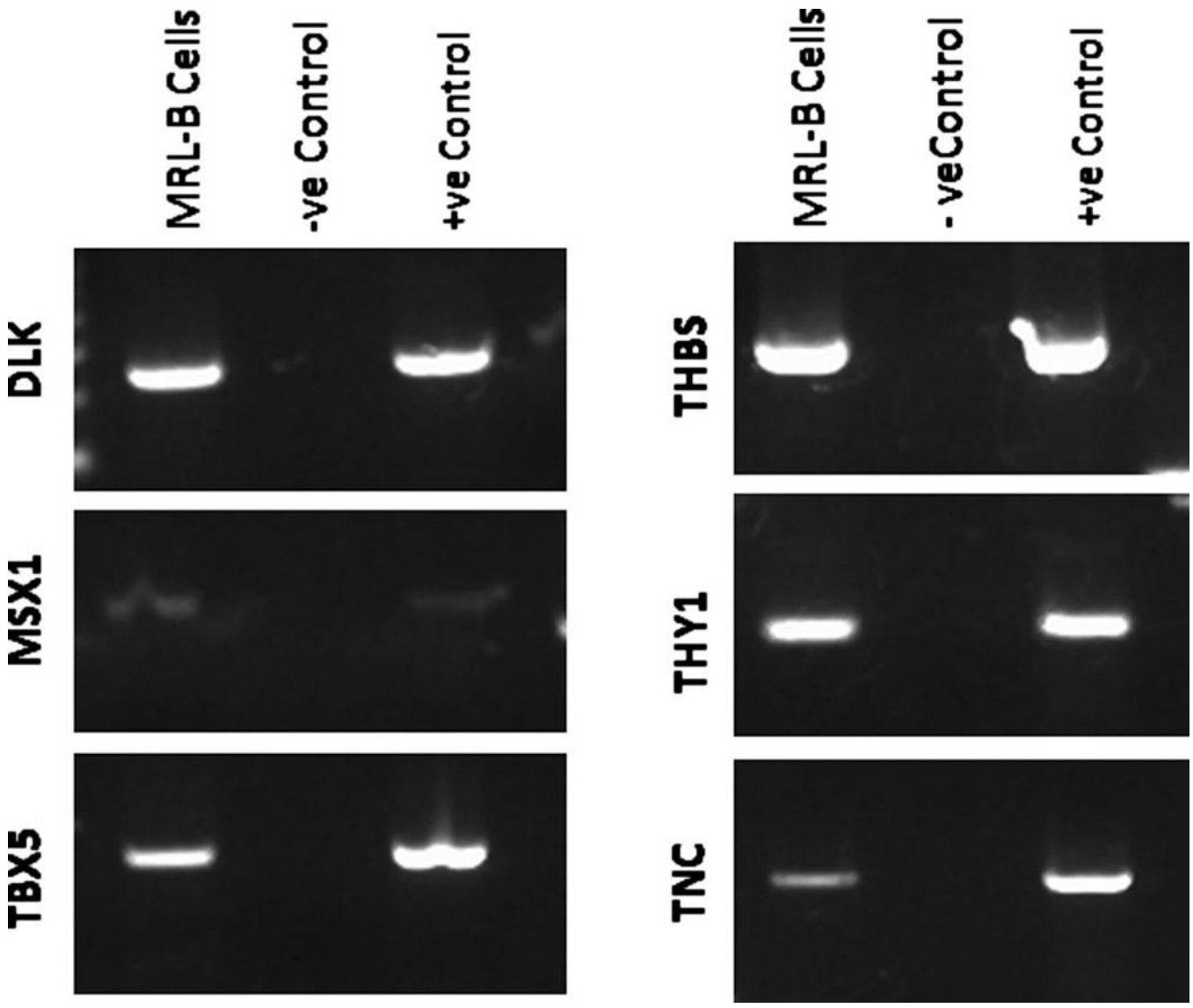


**FIG. 2.**

Images showing gene expression in MRL-B cells at passage 14 and tissue controls. RNA was extracted and transcribed, and the subsequent cDNA screened via PCR for *Tbx5, MSX-1, DLK*, tenascin C, *Thy-1*, and thrombospondin. All samples tested positive for housekeeping gene *GAPDH* (data not shown).

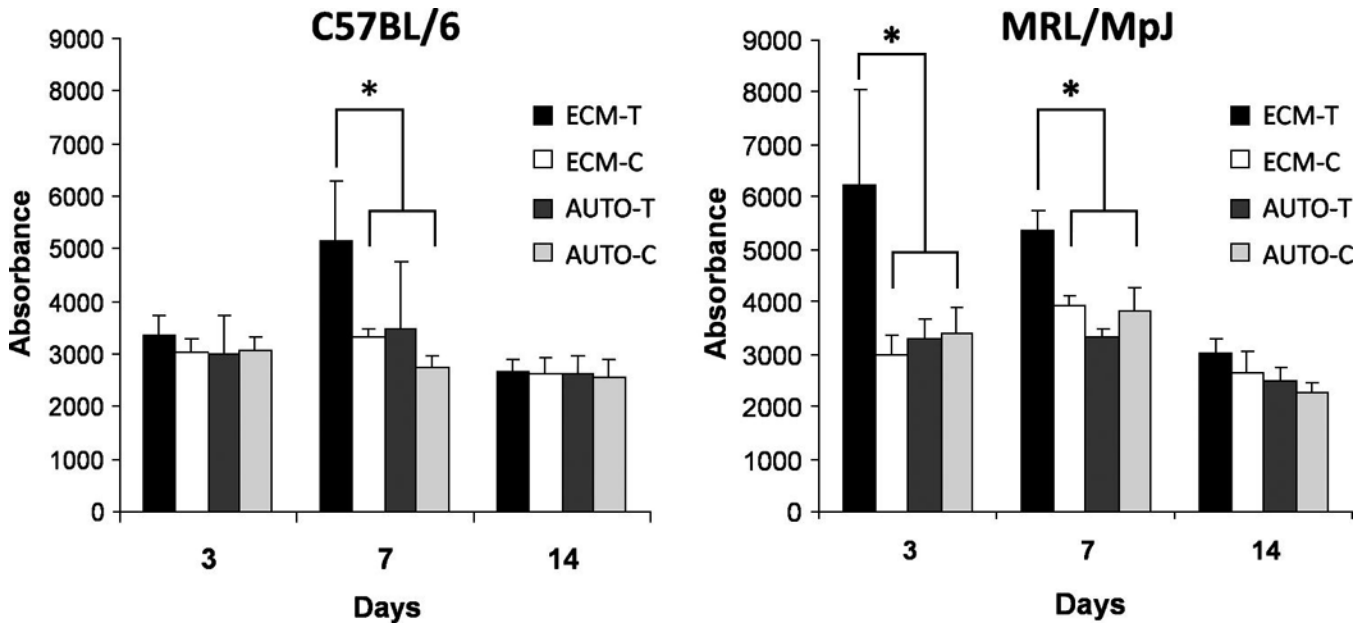


**FIG. 3.**

Graphs showing progenitor cell migration, represented as absorbance, toward tendons excised from C57BL/6 mice (left) and MRL mice (right) 3, 7, and 14 days following surgery for each experimental condition: UBM repair (ECM-T), normal tendon from mouse receiving UBM scaffold (ECM-C), autologous repair (AUTO-T), and normal tendon from the mouse that received the autologous repair (AUTO-C). The results are the mean value ($n$=6) ±the standard deviation with asterisk (*) representing $p$<0.05.

**Table 1**

Experimental and Control Conditions for the Present Study

| Test article | Acronym |
|---|---|
| Tendon repaired with UBM–ECM scaffold | ECM-T |
| Normal tendon from mouse with UBM repair | ECM-C |
| Tendon repaired with autologous scaffold | AUTO-T |
| Normal tendon from mouse with autologous scaffold repair | AUTO-C |

## Table 2

Sequences of Murine-Specific Primer Sets Used in Polymerase Chain Reaction

| Gene | Sequence (5′–3′) | Band size (bp) | + Control | − Control |
|---|---|---|---|---|
| Tbx-5 | F: ATATTGTTCCCGCAGACGACCACA<br>R: TAATGTGTCCAAACGGGTCCAGGT | 200 | Heart | Brain |
| Dlk | F: ACAATGTCTGCAGGTGCCATGTTG<br>R: AGGAGCATTCGTACTGGCCTTTCT | 224 | NIH-3T3 | Heart |
| Msx-1 | F: CTCTCGGCCATTTCTCAGTC<br>R: TACTGCTTCTGGCGGAACTT | 246 | Brain | NIH-3T3 |
| THBS | F: ATCGCGAAGCTGCTATCCAGTTCT<br>R: TCTTCATCTGCCTCAAGGAAGCCA | 457 | NIH-3T3 | Heart |
| TnC | F: CGGATCCGTTTGGAGACCGCAGAGAAGAA<br>R: CGCAAGCTTTGTCCCCATATCTGCCCATCA | 365 | NIH-3T3 | Spleen |
| Thy-1 | F: CAAGGTCCTTACCCTAGCCAA<br>R: CCAGCTTGTCTCTATACACACTG | 125 | NIH-3T3 | Lung |
| GAPDH | F: CGCAACGACCCCTTCATTGACC<br>R: CGATGAGCCCTTCCACAATGCC | 432 | | |